

## **At-sea experiment of adaptive time-reversal multiuser communication in the deep ocean**

Takuya Shimura\*, Yukihiro Kida, Mitsuyasu Deguchi, Yoshitaka Watanabe, and Hiroshi Ochi

*Marine Technology Development Department, Japan Agency for Marine-Earth Science and Technology, Yokosuka, Kanagawa 237-0061, Japan*

E-mail: acoustic237@jamstec.go.jp

An at-sea experiment of multiuser communication in deep water using adaptive time reversal was carried out. In the experiment, two sources and a 20-channel receiver array were deployed at the range of 30 km in an area of 1500 - 2000 m water depth. One of the sources was moored and the other was suspended at various depths. For processing signals actually transmitted from two sources, it was demonstrated that adaptive time reversal could cancel multiuser interference independently of relative source positions. Additionally, for a more detailed investigation, the analysis of multiuser test signals by synthesizing signals from different depths was performed. As a result, especially in the case of adjacent sources, adaptive time reversal significantly suppressed crosstalk.

## 1. Introduction

Recently, in the field of underwater acoustic communication, demands for multiuser communication have increased for communication with multiple autonomous underwater vehicles (AUVs) or underwater acoustic communication networks.<sup>1-8)</sup> Time reversal is an attractive solution to achieving such communication.<sup>5-11)</sup> Originally, even in the case of single-user communication, time reversal is suitable for underwater acoustic communication in terms of countermeasures to intersymbol interference (ISI) due to a rich multipath environment inherent in ocean acoustic propagation. Spatial and temporal focusing of time reversal removes such ISI by collecting multipath signals. Namely, time reversal can turn the disadvantages of multipath signals into advantages. Moreover, time reversal can be easily extended to multiuser communication by the same processing as in the single user case without sacrificing throughput.

As other candidates for multiuser communication, code-division multiple access (CDMA)<sup>12-17)</sup> or orthogonal frequency-division multiplexing (OFDM)<sup>18-24)</sup> are well known. In the case of CDMA, data symbols are spread with some orthogonal codes to discriminate different users. In the case of OFDM, which is basically packet communication, it is easier to change the frequency band assigned to each user flexibly than in CDMA, so that the total frequency usage efficiency is improved by reducing waste in the frequency band on a moment-to-moment basis. However, in these methods, total traffic capacity is divided by the number of users; then, the data transmission rate for each user is sacrificed. Additionally, in these methods, preparatory communication to establish a communication channel is necessary. In uplink with CDMA, signals from users must be received simultaneously to maintain code orthogonality. Then, it is necessary to control the timing of transmissions from users. In using OFDM, the base station and users must communicate and decide the packet structure in frequency and time before sending information-bearing signals. In underwater acoustic communication, unlike in radio communication in air, the available bandwidth and source level are tightly limited, as is known well. Thus, such methods that require preparatory communication to establish a communication channel are not preferred.

In contrast to such disadvantages, in time-reversal communication, it is not necessary to care about signal collision in communication from multiple users. Time-reversal spatial focusing can separate signals from sources at different positions by the same processing for single users. Thus, time-reversal multiuser communication is a type of space division multiplexing (SDM) method, and communication for communication as mentioned above is not required. Thus, it is appropriate for multiuser underwater acoustic communication.

In this study, adaptive time reversal<sup>25-27)</sup> is introduced to additionally enhance crosstalk mitigation. With adaptive time reversal, signals from undesired users are suppressed while signals from the desired user are maintained. In the spatial response of adaptive time reversal, the null point is generated at the position of undesired users. Thus, adaptive time reversal gives better crosstalk cancellation performance.

In this paper, results of an at-sea experiment for multiuser communication in the deep ocean are described, in which two source were used. The relative positions of these sources were changed to investigate the effect of multiuser interference. As a result, especially when sources are close together, adaptive time reversal is significantly effective for suppressing multiuser interference. The scope of this study is communication from multiple sources (users) to a receiver array (base station). Thus, only multiuser, single-input-multiple-output (SIMO) communication, that is, uplink communication, is discussed.

## **2. Adaptive time-reversal multiuser communication**

### **2.1 Time-reversal communication**

Time reversal for SIMO communication is called passive time reversal<sup>28)</sup> in contrast to active time reversal<sup>29)</sup> for multi-input-single-output (MISO) communication. In the case of active time reversal, time-reversal signals are modulated with information-bearing symbols and actually transmitted from an array to a focus point. On the other hand, in passive time reversal, similar spatial and temporal focusing effects can be obtained by signal processing on the receiver array side. As mentioned above, the objective of this study is to investigate multiuser communication from multiple sources such as AUVs to a receiver array (base station). Thus, only passive time reversal is discussed hereafter, except in Sect. 2.3, and is sometimes referred to as only “time reversal” without mentioning “passive” explicitly.

In passive time reversal, a probe signal is transmitted from a source, followed by an information-bearing signal. The channel response from the source to the receiver array is obtained from the received probe signal, which is cross-correlated with the received information-bearing signal at each channel, and the resultant signals are summed over the channels. This process is equivalent to the active time-reversal process. Therefore, through time reversal spatial and temporal focusing effects, in addition to the removal of ISI, signals from sources at different positions can be separated, as shown in Fig. 1. Because the information-bearing signal, which is convolved by the same channel response, can be extracted by the process of cross-correlation.

### **2.2 Adaptive time reversal**

As mentioned above, time reversal can be extended to communication with multiple users without additional signal processing. However, in some cases, it is difficult to separate users, especially when the sources are in the vicinity of each other. Thus, in order to enhance crosstalk mitigation, adaptive time reversal is applied in this study, as was proposed by Kim et al.<sup>25)</sup> Its theory is explained here briefly for the case of two users.

For the channel response,  $h_j^i(t)$ , from the  $i$ th source (user) to the  $j$ th element of the receiver array and its expression in the frequency domain,  $H_j^i(f)$ , a vector  $\mathbf{d}_k$  is defined as

$$\mathbf{d}_k = [H_1^k(f) \cdots H_M^k(f)]^T, \quad (1)$$

where  $M$  is the total number of receivers.

To suppress crosstalk, an adaptive time-reversal signal for user 1  $\mathbf{w}_1$  is given by

$$\mathbf{w}_1 = \frac{\mathbf{R}^{-1}\mathbf{d}_1}{\mathbf{d}_1^\dagger \mathbf{R}^{-1} \mathbf{d}_1}, \quad (2)$$

where

$$\mathbf{R} = \mathbf{d}_1 \mathbf{d}_1^\dagger + \mathbf{d}_2 \mathbf{d}_2^\dagger + \sigma^2 \mathbf{I}, \quad (3)$$

subject to the constraint that

$$\mathbf{w}_1^\dagger \mathbf{d}_1 = 1. \quad (4)$$

Here,  $\dagger$  denotes the complex conjugate transpose and  $\sigma^2 \mathbf{I}$  is a small diagonal loading for a matrix inversion with an identity matrix  $\mathbf{I}$ . Similarly, an adaptive time-reversal signal for user 2  $\mathbf{w}_2$  can be derived in Eq. (2) by substituting  $\mathbf{d}_1$  with  $\mathbf{d}_2$ . By calculating Eq. (2) for all frequencies in the bandwidth and converting them to the time domain, an adaptive time-reversal signal can be obtained. The adaptive time-reversal signal ( $\mathbf{w}$ ) is converted again to the time domain expression and replaces the received probe signals, which are correlated with the received information-bearing signals, in conventional passive time reversal. Hereafter, to clearly distinguish adaptive time reversal (ATR), only time reversal without adaptive is described as the “conventional” time reversal (CTR). In this study, after time-reversal processing, a single-channel decision feedback equalizer (DFE) with a small number of taps is applied to remove residual ISI, similarly as in previous studies.<sup>10,11)</sup>

### 2.3 Spatial crosstalk suppression effect by ATR

Before analyzing experimental data, to explain the spatial crosstalk suppression effect by ATR, simulation results obtained by the normal mode method are shown in this section. Assume that two sources are located at the points  $(r, z)=(40, 45)$  and  $(60, 55)$  (m) in the

Pekeris waveguide as a simple basic model, as shown in Fig. 2, where  $r$  and  $z$  are the range and depth in the cylindrical coordinate, respectively. The water depth is 100 m, the range between the focal points and the time-reversal array is 15 km, and the frequency is 500 Hz. The acoustic pressure fields when conventional and adaptive time-reversal signals, which are supposed to be focused at each point, are transmitted from the array, are shown in Fig. 3. The left and right panels show the focusing fields to points (40, 45) and (60, 55), respectively. Note that the pressures indicated in these panels are normalized by the maximum pressure in each panel. The upper panels show the results for CTR. In these panels, it is shown that time-reversal signals converge to the original source point, while they interfere with each other's focal point, as indicated by white circles. Such interference causes multiuser crosstalk in communication when signals from two users collide. On the other hand, in the results of ATR, as shown in the lower panels, null points are clearly generated to each other's focal point. This is the crosstalk cancellation effect of ATR. Although these are ideal results with active time reversal in an ideal simple model, they are analogous to those of passive time reversal for communication.

### 3. Experimental methods

An at-sea experiment was carried out in area whose water depth was approximately from 1500 to 2000 m in Suruga Bay, as shown in Fig. 4. Two low-frequency sources, whose source level is 196 dB approximately in the bandwidth from 450 to 550 Hz, and a twenty-channel receiver array, whose intervals between receivers were 6 m, were used in this experiment. One of the sources was suspended from the research vessel at various depths from 300 to 1100 m, and the other source was moored at the depth of 600 m, several kilometers away from the suspended source. These suspended and moored sources are indicated as Tx1 and Tx2, respectively in this order, hereafter. The receiver array was also moored approximately 30 km away from the sources, as shown in Fig. 4, that is, the receiver array aperture spanned depths from 840 to 954 m. The sound speed profile (left panel) and bathymetry (right panel) at the experiment site are also shown in Fig. 4.

In this experiment, the information-bearing signals, which comprise 2048 symbols modulated with binary phase shift keying (BPSK) and quadrature phase shift keying (QPSK) at a rate of 100 symbols/s, were transmitted. The initial 200 symbols were treated as training symbols for DFE.

In this experiment, two types of measurements, coinstantaneous transmissions from Tx1 and Tx2 and single transmissions from Tx1, were carried out. In the former, the two

sources transmitted signals including different information-bearing signals modulated with BPSK or QPSK at almost the same time. The multiuser-interfered parts of the received signals were analyzed, as described in Sect. 4.1. In the latter, only Tx1 actually transmitted signals and signals from different positions were synthesized to simulate multiuser-interfered signals. These synthesized multiuser signals are also analyzed as described in Sect. 4.2.

## 4. Results and discussion

### 4.1 Analysis with actual multiuser-interfered signals

As mentioned above, the results of analyzing actual multiuser-interfered signals are described in this section. Tx1 and Tx2 transmitted different information-bearing signals modulated with BPSK or QPSK at almost the same time. As explained before, Tx1 was suspended from the research vessel at various depths from 300 to 1100 m, while Tx2 was moored, that is, fixed at the depth of approximately 600 m.

Figure 5 shows the results in the case of BPSK. The horizontal axis and vertical axis indicate the depth of Tx1 and output signal-to-noise ratio (SNR) of Tx1, respectively. Figure 6 shows the results in the case of QPSK similarly. In these figures, input SNRs are also shown for reference. These results show that ATR has better performance than CTR independently of relative positions between the two sources. In some cases of QPSK with CTR, some symbol errors occurred; however, excluding such cases, demodulation with no error could be achieved even for CTR. In all cases, ATR yields improvement of 2 – 5 dB compared with CTR, and realizes multiuser communication with no error.

### 4.2 Analysis with synthesized multiuser-interfered signals

For a more detailed study of the effect of relative source positions, the analysis of synthesized multiuser-interfered signals was carried out. As mentioned above, Tx1 transmitted BPSK and QPSK signals at depths from 300 to 1100 m, as shown in Fig. 3. Thus, BPSK and QPSK signals from various positions were synthesized to simulate multiuser signals in a round-robin manner for every combination. These synthesized signals were demodulated with conventional and adaptive time reversals similarly to the experiment described in the previous section.

Figure 7 shows demodulation results for every synthesized signal combination. Here, BPSK and QPSK signals are treated as signals from different users, such as user1 and user2, respectively. In these graphs, the output SNRs of user1 (BPSK) are plotted, and the QPSK signal of the other user (user2) acts as interference. The depth of user2 is indicated

by vertical dotted lines, whereas the depth of user1 is indicated on the horizontal axis. The vertical axis indicates the difference of the output SNRs of user1 in the case of demodulating synthesized multiuser signals with adaptive and conventional time reversals from output SNRs in the case of demodulating only the user1 signal, before synthesis, with CTR. Thus, it shows how performance is degraded from that of the single user case without multiuser interference. In these figures, output SNRs demodulated with a single-user multichannel DFE (SU-MDFE)<sup>30,31)</sup> are also plotted for comparison as a conventional method, which is a competitor to conventional passive time reversal in single-user SIMO communication.

From this figure, ATR outperforms CTR and SU-MDFE in all cases. The output SNRs with ATR are approximately 0 dB. This means that ATR removes multiuser interference almost completely. On the other hand, output SNRs with CTR are approximately 2 - 4 dB lower than those with ATR. The information-bearing signals, which are random sequence signals, are superimposed, so that the results of 3 dB degradation are reasonable. SU-MDFE, in most cases, is inferior to CTR. It is most important that, even when the depths of two users are the same, the performance of ATR does not deteriorate very much, while the performances of time reversal or SU-MDFE are affected considerably by multiuser interference. Thus, it was found that ATR is significantly effective when source positions are very close to each other.

In Figs. 8 and 9,  $q$ -functions are shown to confirm multiuser interference suppression by ATR, especially when source positions are very close to each other. Figure 8 shows  $q$ -functions in the case that user1 and user2 are at the depths of 307 and 1105 m, respectively, and Fig. 9 shows  $q$ -functions when user1 and user2 are at the depths of 1106 and 1105 m, respectively. The  $q$ -function is defined as the correlation between time-reversal probe signals<sup>8)</sup>, which is an index expressing the time-reversal focusing performance. In single-user communication, if the  $q$ -function shape is an ideal single pulse, time reversal suppresses intersymbol interference successfully. In multiuser communication, the  $q$ -function between different users, that is, cross-correlation between time-reversal signals for different users, indicates how multiuser interference exists. In these figures,  $h$  indicates CTR probe signals while  $w$  indicates ATR probe signals, as explained in Sect. 2.2. Therefore,  $h_1h_2$  expresses how user2 interferes with user1 in CTR. In contrast,  $h_1w_2$  expresses how such interference from user2 to user1 is suppressed by ATR. Note that the amplitude of these  $q$ -functions are normalized by the maximum value of  $h_1h_1$  or  $h_2h_2$ , and it should be noted that the vertical axis in  $h_1h_2$  and  $h_1w_2$  is adjusted, that is, it is not the same as in the other panels. From the results of  $h_1h_2$  in Fig. 8, when user1 and user2 are positioned far from each

other, multiuser interference is not clearly observed. On the other hand, from the results of  $h1h2$  in Fig. 9, a peak pulse, whose level is approximately 50% in  $h1h1$  and  $h2h2$ , is clearly observed which causes critical multiuser interference. However, from the results of  $h1w2$ , such interference signals are effectively mitigated. These are the reasons why ATR can realize multiuser communication even when the source positions are located close to each other, as shown in Fig. 7. For reference, such improvement in q-functions are observed similarly with other combinations of source positions.

## 5. Conclusions

ATR was applied to multiuser communication and was demonstrated in the at-sea experiment in the deep ocean. In the analysis of actual multiuser-interfered signals from two sources, it was verified that ATR achieves multiuser communication. Additionally, in the analysis of synthesized multiuser-interfered signals, in which relative positions between the two sources were varied, ATR had the significant effect of separating crosstalk, especially when the two sources were very close to each other, that is, almost at the same position. This feature is expected to be applied in communication with a larger number of multiusers.

As a future work, comparison with other multiuser communication methods will be carried out. Moreover, at-sea experiments at a longer range will be conducted taking into consideration the Doppler effect due to moving sources.

## Acknowledgments

This research is partially supported by a 2013 Grant-in-Aid for Young Scientists (B) (Grant No. 22760645) from the Ministry of Education, Culture, Sports, Science and Technology, Japan. We deeply thank a support staff member in our research group, Takami Mori, the crews of the R/V Kaiyo, and the research assistants of Marine Works Japan Ltd. for their cooperation in the experiment. We sincerely appreciate Heechun Song who proposed the adaptive time-reversal theory and was a host researcher for the first author's visiting research program at the Scripps Institute of Oceanography.



## References

- 1) S. Qader, C. Tsimenidis, M. Johnston, and B. S. Sharif, Proc. Int. Conf. Exhib. Underwater Acoustics, 2014, p. 1233.
- 2) S. Qader, C. Tsimenidis, B. Sharif, and M. Johnston, Proc. Sensor Processing for Defence, 2012, p. 1.
- 3) G. Qiao and J. Zhang, Proc. Int. Conf. Exhib. Underwater Acoustics, 2014, p1477.
- 4) K. G. Kebkal, V. K. Kebkal, O. G. Kebkal, and R. Petroccia, Proc. Int. Conf. Exhib. Underwater Acoustics, 2014, p1181.
- 5) S. Cho, H. C. Song, and W. S. Hodgkiss, J. Acoust. Soc. Am. **133**, 880 (2013).
- 6) S. Cho, H. C. Song, and W. S. Hodgkiss, J. Acoust. Soc. Am. **132**, 5 (2012).
- 7) S. Cho, H. C. Song, and W. S. Hodgkiss, J. Acoust. Soc. Am. **131**, EL163 (2012)
- 8) T. Shimura, H. Ochi, and H. C. Song, J. Acoust. Soc. Am. **134**, 3223 (2013).
- 9) H. C. Song, J. Acoust. Soc. Am. **134**, 2623 (2013).
- 10) T. Shimura, Y. Watanabe, H. Ochi, and H. C. Song, J. Acoust. Soc. Am. **132**, EL49 (2012).
- 11) T. Shimura, H. Ochi, Y. Watanabe, and T. Hattori, Jpn. J. Appl. Phys. **49**, 07HG11 (2010).
- 12) M. Palmese and A. Trucco, Proc. ECUA2012, 2012, p. 731.
- 13) E. C. Page and M. Stojanovic, IEEE J. Oceanic Eng. **33**, 502 (2008).
- 14) M. Stojanovic and L. Freitag, IEEE J. Oceanic Eng. **31**, 685 (2006).
- 15) T. C. Yang and W. Yang, J. Acoust. Soc. Am. **126**, 220 (2009).
- 16) M. Stojanovic and L. Freitag, Proc. Oceans'05, 2005, p. 74.
- 17) E. C. Page, and M. Stojanovic, Proc. Oceans'05, 2005, p. 226.
- 18) T. Hai, Y. Matsuda, T. Suzuki, and T. Wada, Proc. Int. Conf. Exhib. Underwater Acoustics, 2014, p. 1227.
- 19) K. Tu, T. Duman, M. Stojanovic, and J. Proakis, IEEE J. Oceanic Eng. **38**, 333 (2013).
- 20) Y. V. Zakharov, A. K. Morozov, and J. C. Preisig, Proc. ECUA2012, 2012, p. 652.
- 21) F.-X. Socheleau, M. Stojanovic, C. Laot, and J.-M. Passerieux, Proc. ECUA2012, 2012, p. 119.
- 22) C. Polprasert, J. Ritcey, and M. Stojanovic, IEEE J. Oceanic Eng. **36**, 514 (2011).
- 23) P. Ceballos and M. Stojanovic, IEEE J. Oceanic Eng. **35**, 635 (2010).
- 24) C. Lin, M. Chen, W. Zhang, J. Park, and J. R. Yoon, Jpn. J. Appl. Phys. **49**, 07HG12 (2010).
- 25) J. Kim, H. C. Song, and W. A. Kuperman, J. Acoust. Soc. Am. **109**, 1817 (2001).
- 26) H. C. Song, J. Acoust. Soc. Am. **135**, EL154 (2014).

- 27) H. C. Song, J. S. Kim, W. S. Hodgkiss, and J. H. Joo, J. Acoust. Soc. Am. **127**, EL19 (2010).
- 28) D. Rouseff, D. Jackson, W. Fox, C. Jones, J. Ritcey, and D. Dowling, IEEE J. Oceanic Eng. **26**, 821 (2001).
- 29) G. Edelmann, T. Akal, W. Hodgkiss, S. Kim, W. Kuperman, and H. C. Song, IEEE J. Oceanic Eng. **27**, 602 (2002).
- 30) Y. Watanabe and H. Ochi, Jpn. J. Appl. Phys. **34**, 3134 (2004).
- 31) M. Stojanovic, J. Catipovic, and J. G. Proakis, J. Acoust. Soc. Am. **94**, 1621 (1993)

## Figure Captions

**Fig. 1.** (Color online) Concept of multiuser communication by passive time reversal.

**Fig. 2.** (Color online) Simulation conditions.

**Fig. 3.** (Color online) Acoustic pressure field focusing to two different points (users) by CTR (upper panels) and by ATR (lower panels). Left panels and right panels show the focusing fields to points (40, 45) and (60, 55), respectively.

**Fig. 4.** (Color online) At-sea experimental set up. Left panel shows sound velocity profile and right panel shows bathymetry between sources and receiver array and their positions.

**Fig. 5.** (Color online) Results of demodulating actual multiuser-interfered signals in the case of BPSK.

**Fig. 6.** (Color online) Results of demodulating actual multiuser-interfered signals in the case of QPSK.

**Fig. 7.** (Color online) Results of demodulating synthesized multiuser-interfered signals.

**Fig. 8.** q-functions when user1 and user2 are located at depths of 307 and 1105 m, respectively.

**Fig. 9.** q-functions when user1 and user2 are located at depths of 1105 and 1106 m, respectively.

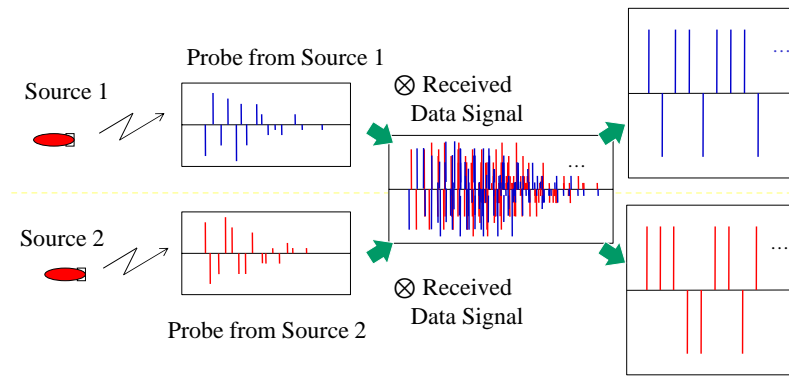


Fig. 1. (Color Online)

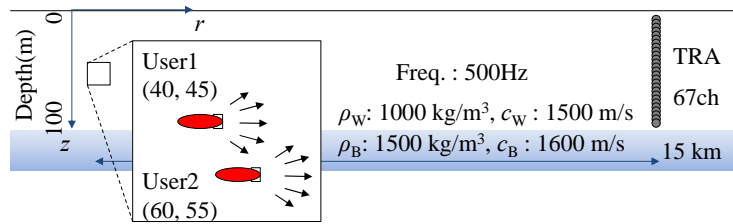


Fig. 2. (Color Online)

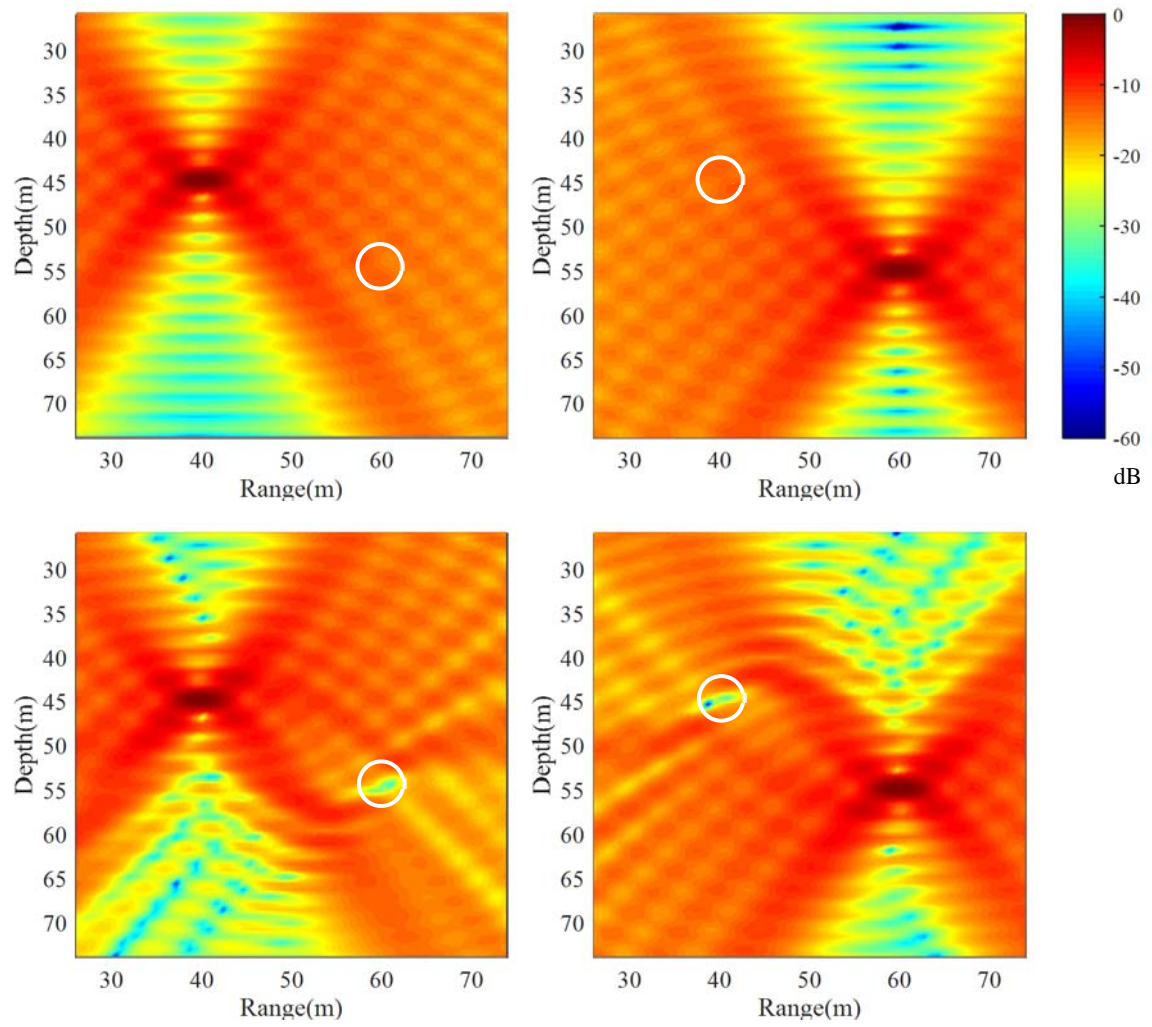


Fig. 3. (Color Online)

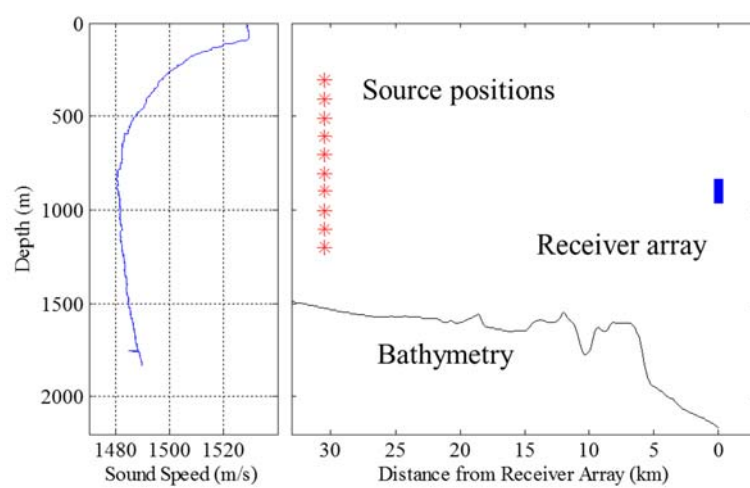


Fig. 4. (Color Online)

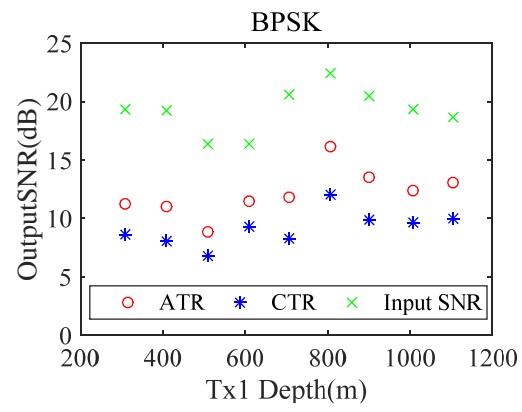


Fig. 5. (Color Online)



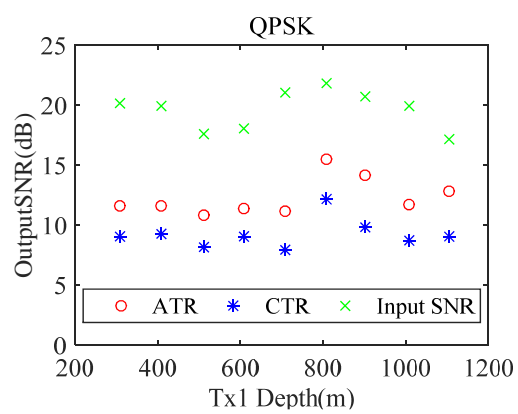


Fig. 6. (Color Online)

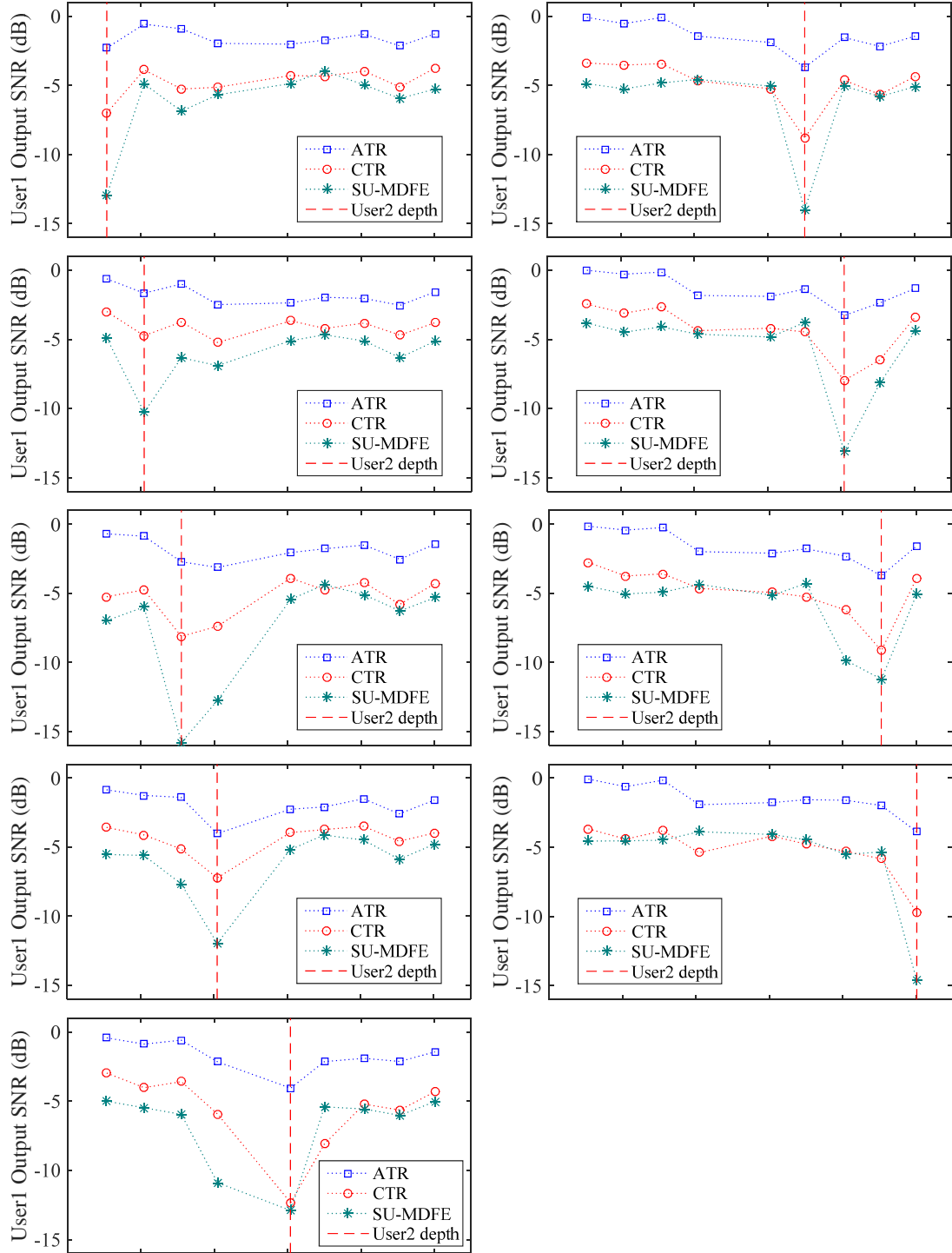


Fig. 7. (Color Online)

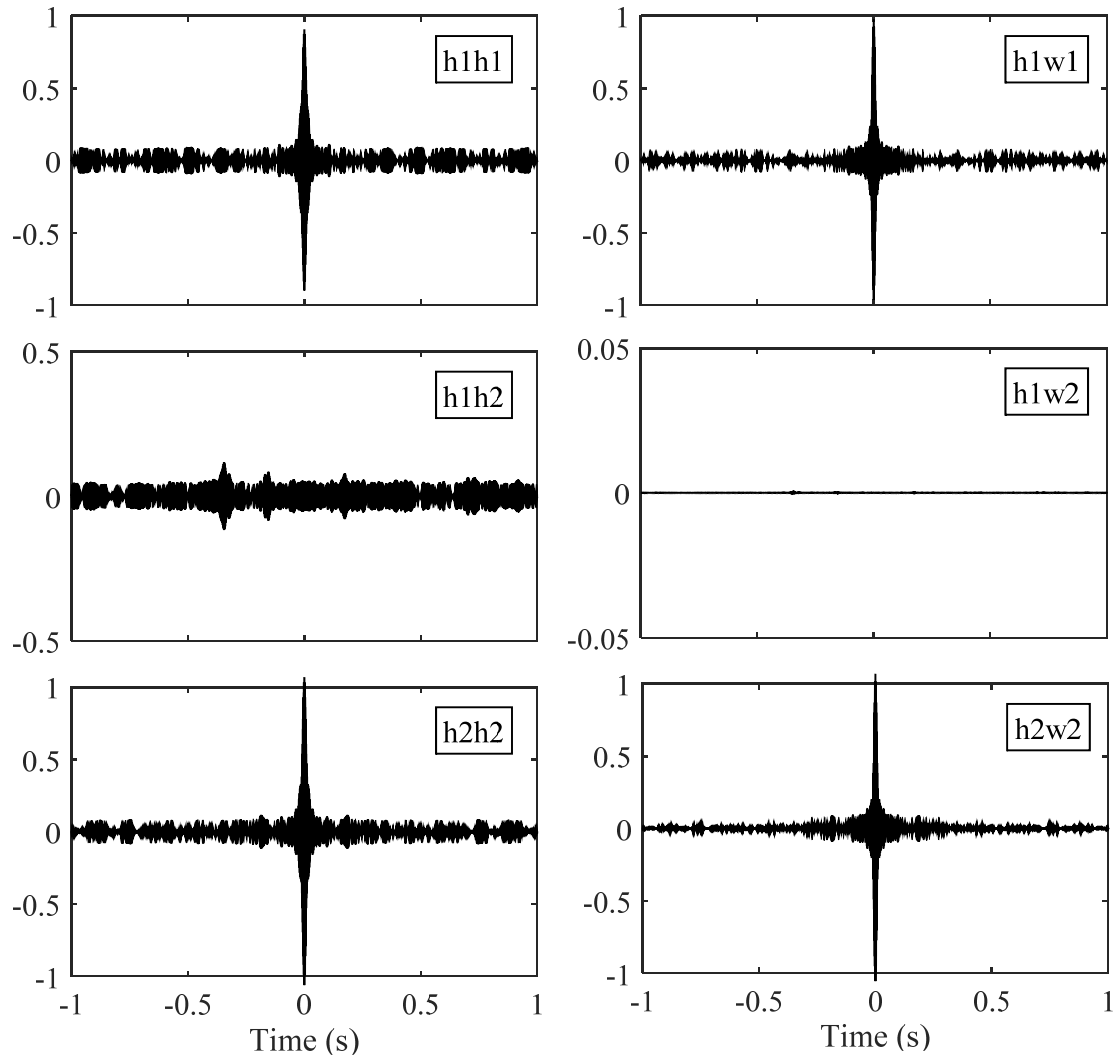


Fig.8.

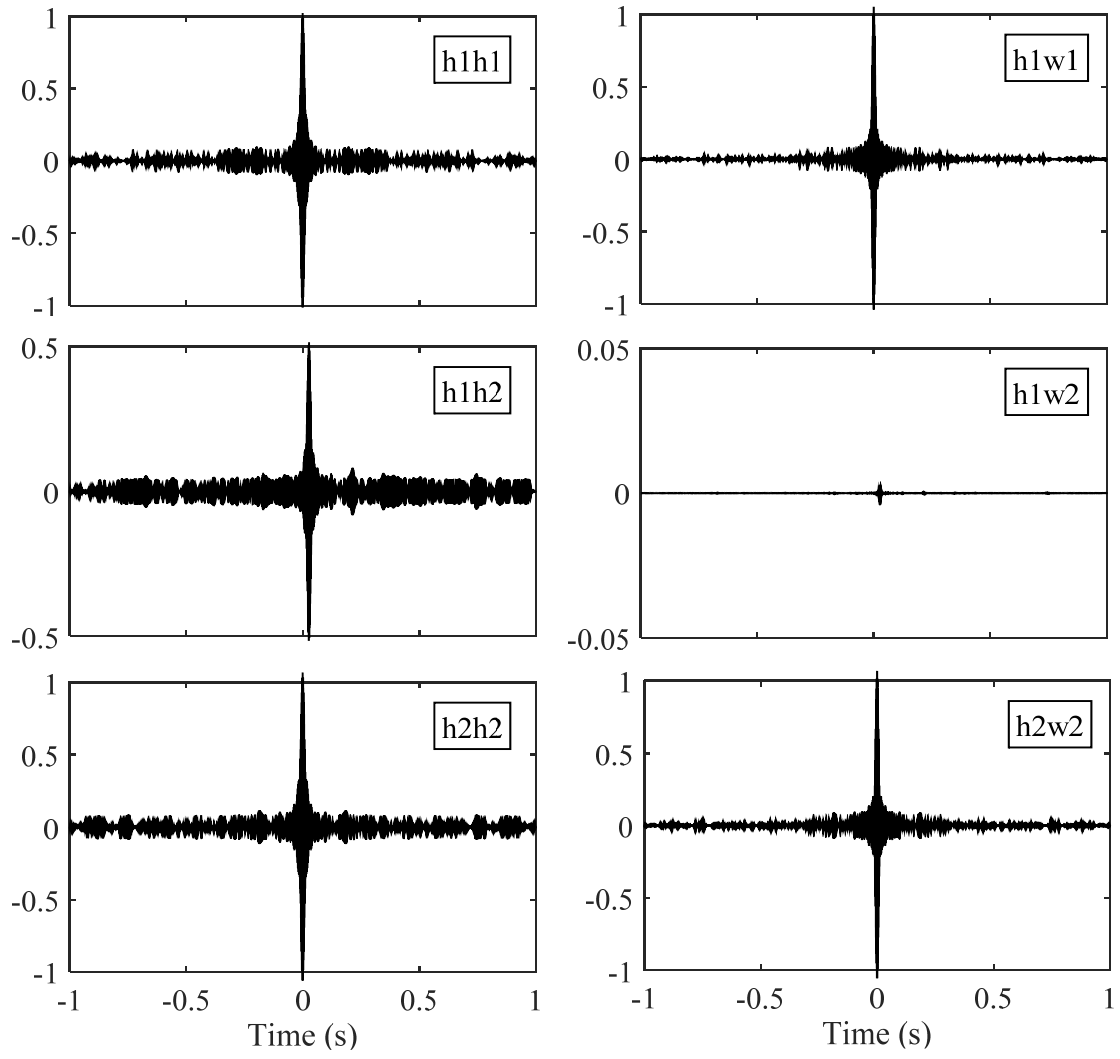


Fig. 9.